DE GRUYTER OPEN

Journal of ELECTRICAL ENGINEERING, VOL 68 (2017), NO2, 109–116

Numerical treatment of the spatio-temporal electromagnetic beam-wave packet

Ľubomír Šumichrast, Jaroslav Franek *

Propagation of a two-dimensional spatio-temporal electromagnetic beam wave is analysed. In parabolic (paraxial) approximation the exact analytical results for a spatio-temporal Gaussian impulse can be obtained. For solution of the full wave equation the numerical simulation has to be used. The various facets of this simulation are discussed here.

K e y w o r d s: electromagnetic wave-packet propagation, parabolic approximation, numerical modeling

1 Introduction

The problem of the total internal reflection on the planar boundary of two dielectric media, as well as of the frustrated total internal reflection in presence of two planar dielectric boundaries, is usually solved for a monochromatic plane wave. To analyse it for monochromatic beam wave, or for the spatio-temporal transient wave-packet, a numerical approach is inevitable. Here some aspects of a numerical treatment of wave propagation are investigated.

We shall consider the propagation of a pulsed two-dimensional spatio-temporal TE-polarised beam wave, with the vector of the electric intensity $\mathbf{E}(x,z,t)$ defined as

$$\mathbf{E}(x,z,t) = \mathbf{u}_y E_y(x,z,t) = \mathbf{u}_y E_0 f(x,z,t), \qquad (1)$$

where $f(x,z,t)$ is the function describing distribution of the wave amplitude in time and space. If the propagation along the z axis is considered, the initial condition - the amplitude distribution $f_0(x,t)$ - must be given in *eg* the plane $z=0$, *ie*

$$f(x,z,t)|_{z=0} = f_0(x,t). \qquad (2)$$

As a first case, let us analyse the monochromatic beam wave with $f(x,z,t) = \mathrm{Re}\{\varphi(x,z)\exp(j\omega_0 t)\}$, *ie*

$$\mathbf{E}(x,z,t) = \mathrm{Re}\left\{\widehat{\mathbf{E}}(x,z)\exp(j\omega_0 t)\right\}, \qquad (3)$$

where $\widehat{\mathbf{E}}(x,z) = \mathbf{u}_y E_0 \varphi(x,z)$. The complex, in x direction spatially-bounded impulse-like, monochromatic amplitude distribution of the wave is given by $\varphi(x,z)$ and ω_0 is the angular frequency of the harmonic oscillations. The initial condition for the complex wave amplitude reads $\varphi(x,z)|_{z=0} = \varphi_0(x)$.

As a second case, the harmonically modulated wave packet will be treated, where

$$f(x,z,t) = \mathrm{Re}\{\psi(x,z,t)\ \exp(j\omega_0 t)\}, \qquad (4)$$

where $\psi(x,z,t)$ is the spatial and temporal impulse-like complex "slowly varying amplitude-envelope in time" of the wave. The initial condition for the complex wave amplitude reads $\psi(x,z,t)|_{z=0} = \psi_0(x,t)$.

2 The wave and the Helmholtz equations governing the propagation effects

The propagation of waves is generally governed by the wave equation in form

$$\frac{\partial^2 f(x,z,t)}{\partial x^2} + \frac{\partial^2 f(x,z,t)}{\partial z^2} - \frac{1}{c^2}\frac{\partial^2 f(x,z,t)}{\partial t^2} = 0, \qquad (5)$$

for the wave amplitude distribution $f(x,z,t)$ in (1), where $c = 1/\sqrt{\mu\varepsilon}$ is the phase velocity of wave propagation in the given lossless medium with permittivity ε and permeability μ.

The complex amplitude $\varphi(x,z)$ of a monochromatic wave in (3) fulfils the Helmholtz equation

$$\frac{\partial^2 \varphi(x,z)}{\partial x^2} + \frac{\partial^2 \varphi(x,z)}{\partial z^2} + \beta_0^2 \varphi(x,z) = 0, \qquad (6)$$

where $\beta_0 = \omega_0/c$ is the phase constant of the harmonic plane wave.

After having introduced the "slowly varying envelope in propagation direction" $\overline{\varphi}(x,z)$ by the substitution $\varphi(x,z) = \overline{\varphi}(x,z)\exp(-j\beta_0 z)$, *ie* by stripping-off the fast oscillations due to term $\exp(-j\beta_0 z)$ from $\varphi(x,z)$, one arrives instead of (6) to the wave equation for $\overline{\varphi}(x,z)$ in the form

$$\frac{\partial^2 \overline{\varphi}(x,z)}{\partial x^2} - 2j\beta_0 \frac{\partial \overline{\varphi}(x,z)}{\partial z} + \frac{\partial^2 \overline{\varphi}(x,z)}{\partial z^2} = 0. \qquad (7)$$

For the "slowly varying envelope in time" $\psi(x,z,t)$ in (4) the time dependent Helmholtz equation reads

$$\frac{\partial^2 \psi}{\partial x^2} + \frac{\partial^2 \psi}{\partial z^2} - \frac{1}{c^2}\frac{\partial^2 \psi}{\partial t^2} - \frac{2j\beta_0}{c}\frac{\partial \psi}{\partial t} + \beta_0^2 \psi = 0. \qquad (8)$$

* Slovak University of Technology, Institute of Electrical Engineering Ilkovičova 3, SK-81219 Bratislava, Slovakia, lubomir.sumichrast@stuba.sk

DOI: 10.1515/jee-2017–0015, Print (till 2015) ISSN 1335-3632, On-line ISSN 1339-309X

If one defines "slowly varying envelope in time and space" $\overline{\psi}(x,z,t)$ similarly as for (7) by $\psi(x,z,t) = \overline{\psi}(x,z,t)\exp(-j\beta_0 z)$, then the time dependent Helmholtz equation (8) takes the form

$$\frac{\partial^2\overline{\psi}}{\partial x^2}+\frac{\partial^2\overline{\psi}}{\partial z^2}-\frac{1}{c^2}\frac{\partial^2\overline{\psi}}{\partial t^2}-2j\beta_0\left(\frac{\partial\overline{\psi}}{\partial z}+\frac{1}{c}\frac{\partial\overline{\psi}}{\partial t}\right)=0. \quad (9)$$

3 Solution for the monochromatic beam wave

After introducing for $\varphi(x,z)$ the spatial Fourier transform pair $\varphi(x,z)\leftrightarrow\Phi(q,z)$ by

$$\Phi(q,z)=\tfrac{1}{2\pi}\int_{-\infty}^{\infty}\varphi(x,z)\exp(jqx)\,\mathrm{d}x, \quad (10)$$

$$\varphi(x,z)=\int_{-\infty}^{\infty}\Phi(q,z)\exp(-jqx)\,\mathrm{d}q, \quad (11)$$

one arrives instead of (6) at the Helmholtz equation in spectral domain

$$\frac{\partial^2\Phi(q,z)}{\partial z^2}+\left(\beta_0^2-q^2\right)\Phi(q,z)=0. \quad (12)$$

The solution for the wave propagating in the positive direction of the z-axis reads [1]

$$\Phi(q,z)=\Phi_0(q)\exp\left(-jz\sqrt{\beta_0^2-q^2}\right), \quad (13)$$

where $\Phi_0(q)$ is the Fourier transform of the initial value $\varphi_0(x)\leftrightarrow\Phi_0(q)$, thus leading to the formula [1]

$$\varphi(x,z)=\int_{-\infty}^{\infty}\Phi_0(q)\exp\left(-jz\sqrt{\beta_0^2-q^2}\right)\exp(-jqx)\,\mathrm{d}q, \quad (14)$$

where $\varphi(x,z)$ is expressed as an integral of the spatial spectrum of plane waves.

Formula (14) describes the expansion of the beam wave into the spectrum of plane waves. To the spectral density of the electric-intensity-vector $\widehat{\mathbf{e}}(q,x,z)$ in form of plane-wave components

$$\widehat{\mathbf{e}}(q,x,z)=\mathbf{u}_y E_0\Phi_0(q)\exp\{-j(qx+kz)\}, \quad (15)$$

where $k=\sqrt{\beta_0^2-q^2}$, pertains the spectral density of the magnetic-intensity-vector $\widehat{\mathbf{h}}(q,x,z)$ in form of plane-wave components equal to

$$\widehat{\mathbf{h}}(q,x,z)=(E_0/\beta_0 Z_0)\left[q\mathbf{u}_z-k\mathbf{u}_x\right]\times \times\Phi_0(q)\exp\{-j(qx+kz)\}, \quad (16)$$

where $Z_0=\sqrt{\mu/\varepsilon}$ is the wave impedance of the lossless medium. Each component of the plane wave spectral density described by (15) and (16) propagates in the direction given by the unit vector

$$\mathbf{n}=\sin\theta\mathbf{u}_x+\cos\theta\mathbf{u}_z,$$

where $\tan\theta=q/k$.

Generally, the spectrum of plane-wave-amplitudes $\Phi_0(q)$ for the given initial-value wave-amplitude-profile $\varphi_0(x)$ may contain also the components with spatial frequencies q higher than β_0. In that case only the waves propagating in x - direction and evanescent in z-direction occur, defined as

$$\widehat{\mathbf{e}}(q,x,z)=\mathbf{u}_y E_0\Phi_0(q)\exp(-\kappa z)\exp(-jqx), \quad (17)$$

$$\widehat{\mathbf{h}}(q,x,z)=(E_0/\beta_0 Z_0)\left[q\mathbf{u}_z-j\kappa\mathbf{u}_x\right]\times \times\Phi_0(q)\exp(-\kappa z)\exp(-jqx), \quad (18)$$

where $\kappa=\sqrt{q^2-\beta_0^2}$ for $q>\beta_0$.

4 Solution for the spatio-temporal electromagnetic wave packet

After introducing for $\psi(x,z,t)$ the two-dimensional spatio-temporal Fourier transform pair $\psi(x,z,t)\Leftrightarrow\Psi(q,z,\Omega)$ by

$$\Psi(q,z,\Omega)= \tfrac{1}{(2\pi)^2}\int_{-\infty}^{\infty}\int_{-\infty}^{\infty}\psi(x,z,t)\exp\{j(qx-\Omega t)\}\,\mathrm{d}x\mathrm{d}t, \quad (19)$$

$$\psi(x,z,t)=\int_{-\infty}^{\infty}\Psi(q,z,\Omega)\exp\{j(\Omega t-qx)\}\,\mathrm{d}q\mathrm{d}\Omega, \quad (20)$$

one arrives instead of (8) at the Helmholtz equation in spatio-temporal spectral domain

$$\frac{\partial^2\Psi(x,z,\Omega)}{\partial z^2}+\left\{(\beta_0+\Omega/c)^2-q^2\right\}\Psi(x,z,\Omega)=0. \quad (21)$$

The solution for the wave propagating in the positive direction of the z-axis now reads

$$\Psi(q,z,\Omega)=\Psi_0(q,\Omega)\exp\left\{-jz\sqrt{(\beta_0+\Omega/c)^2-q^2}\right\}, \quad (22)$$

where $\Psi_0(q,\Omega)$ is the Fourier transform of the initial value $\psi_0(x,t)\Leftrightarrow\Psi_0(q,\Omega)$, thus leading to the formula

$$\psi(x,z,t)= \int_{-\infty}^{\infty}\int_{-\infty}^{\infty}\Psi_0(q,\Omega)\exp\left(-jz\sqrt{[\beta_0+\Omega/c]^2-q^2}\right)\times \times\exp\{j(\Omega t-qx)\}\,\mathrm{d}q\mathrm{d}\Omega, \quad (23)$$

where $\psi(x,z,t)$ is expressed as an twofold-integral of the spatio-temporal spectral density $\Psi(q,z,\Omega)$.

Similarly as for (14), the formula (23) describes the expansion of the beam wave into the spectrum of plane waves. The complex-amplitude electric-intensity-vector spectral density $\widehat{\mathbf{e}}(q,x,z,t)$ has again the form of a plane wave

$$\widehat{\mathbf{e}}(q,x,z,t) = \mathbf{u}_y E_0 \Psi_0(q,\Omega) \exp\{-j(qx+kz)\} \times \\ \times \exp\{j(\omega_0+\Omega)t\}, \tag{24}$$

with pertaining magnetic-intensity-vector equal to

$$\widehat{\mathbf{h}}(q,x,z,t) = [E_0/(\beta_0+\Omega/c)\, Z_0]\,[q\mathbf{u}_z - k\mathbf{u}_x] \times \\ \Psi_0(q,\Omega) \exp\{-j(qx+kz)\} \exp\{j(\omega_0+\Omega)t\}, \tag{25}$$

where $k(\Omega) = \sqrt{(\beta_0+\Omega/c)^2 - q^2}$, propagating in the direction given by the unit vector (now depending also on Ω) $\mathbf{n}(\Omega) = \sin\theta\mathbf{u}_x + \cos\theta\mathbf{u}_z$, where $\tan\theta(\Omega) = q/k$.

5 Parabolic (paraxial) approximation

If the spatial spectrum $\Phi_0(q)$ in (14) consists only of spectral components with spatial frequencies fulfilling the condition $q << \beta_0$, then the "low spatial frequency" approximation can be used

$$\sqrt{\beta_0^2 - q^2} \approx \beta_0 - q^2/2\beta_0, \tag{26}$$

and instead of (14) one arrives at the inverse Fourier transform formula in the form

$$\varphi(x,z) = \exp(-j\beta_0 z) \times \\ \times \int_{-\infty}^{\infty} \Phi_0(q) \exp\left(jq^2 z/2\beta_0\right) \exp(-jqx)\,\mathrm{d}q. \tag{27}$$

Observe that the integral in (27) is the "slowly varying envelope in propagation direction" $\overline{\varphi}(x,z)$ as defined above, $\varphi(x,z) = \overline{\varphi}(x,z)\exp(-j\beta_0 z)$. The integral in (27) is in fact the solution of the following equation in the spatial-frequency domain

$$\frac{\partial\overline{\Phi}(q,z)}{\partial z} - \frac{jq^2}{2\beta_0}\overline{\Phi}(q,z) = 0 \tag{28}$$

for $\overline{\varphi}(x,z) \leftrightarrow \overline{\Phi}(q,z)$ with the initial condition $\overline{\Phi}(q,z)\big|_{z=0} = \Phi_0(q)$. The transformation of (28) into the spatial domain yields the parabolic partial differential equation

$$\frac{\partial^2\overline{\varphi}(x,z)}{\partial x^2} - 2j\beta_0\frac{\partial\overline{\varphi}(x,z)}{\partial z} = 0 \tag{29}$$

for $\overline{\varphi}(x,z)$. It approximates (7), where the last term can be neglected since $|\partial\overline{\varphi}/\partial z| << \beta_0$ due to the "slowly varying envelope" principle.

Hence the nature of paraxial approximation can be explained in spatial frequency domain by "low-spatial frequency" approximation (26), or in spatial domain by parabolic approximation (29) of the exact equation (7).

Parabolic approximation can be used also for spatio-temporal wave packet. If the spatio-temporal spectral density $\Psi(q,z,\Omega)$ contains only spectral components with frequencies fulfilling the condition $\Omega << \omega_0$ and with the spatial frequencies fulfilling the condition $q << \omega_0/c$, then the "low temporal and spatial frequency" approximation

$$\sqrt{(\beta_0+\Omega/c)^2 - q^2} \approx \beta_0 + \frac{\Omega}{c} + \frac{\Omega^2}{2c^2\beta_0} - \frac{q^2}{2\beta_0} \tag{30}$$

can be similarly used, yielding instead of (23) the result in the retarded form

$$\psi(x,z,t-z/c) = \psi(x,z,\tau) = \exp(-j\beta_0 z) \times \\ \times \int_{-\infty}^{\infty}\int_{-\infty}^{\infty} \Psi_0(q,\Omega) \times \exp\left\{\frac{jz}{2\beta_0}\left[q^2 - (\Omega/c)^2\right]\right\} \\ \times \exp\{j[\Omega(t-z/c) - qx]\}\,\mathrm{d}q\mathrm{d}\Omega, \tag{31}$$

where $\tau = t - z/c$.

The first term in (31) together with $\exp(j\omega_0 t)$ term in (4) yields $\exp\{j\omega_0(t-z/c)\}$ *ie* the retarded harmonic-oscillations of the carrier wave propagating along z-axis with the velocity c.

Observe that the integral in (31) is the "slowly-varying-envelope in time and space" $\overline{\psi}(x,z,t)$ as defined above, $\psi(x,z,t) = \overline{\psi}(x,z,t)\exp(-j\beta_0 z)$.

The integral in (31) is in fact the solution of the following equation in the spatio-temporal frequency-domain

$$\frac{\partial\overline{\Psi}(q,z,\Omega)}{\partial z} - j\left\{\frac{q^2}{2\beta_0} - \frac{\Omega^2}{2\beta_0 c^2} - \frac{\Omega}{c}\right\}\overline{\Psi}(q,z,\Omega) = 0, \tag{32}$$

for $\overline{\psi}(x,z,t) \Leftrightarrow \overline{\Psi}(q,z,\Omega)$ with the initial condition $\psi_0(x,t) \Leftrightarrow \Psi_0(q,\Omega)$. This corresponds to the parabolic equation

$$\frac{\partial^2\overline{\psi}}{\partial x^2} - 2j\beta_0\frac{\partial\overline{\psi}}{\partial z} - \frac{1}{c^2}\frac{\partial^2\overline{\psi}}{\partial t^2} - \frac{2j\beta_0}{c}\frac{\partial\overline{\psi}}{\partial t} = 0 \tag{33}$$

for $\overline{\psi}(x,z,t)$ in the spatio-temporal domain that approximates the equation (9), where the term $\partial^2\overline{\psi}/\partial z^2$ has been neglected with the same argument as in (29).

For the retarded time $\tau = t - z/c$ and $\overline{\psi}(x,z,\tau) = \overline{\psi}(x,z,t-z/c)$ the resulting parabolic equation instead of (33) reads

$$\frac{\partial^2\overline{\psi}(x,z,\tau)}{\partial x^2} - 2j\beta_0\frac{\partial\overline{\psi}(x,z,\tau)}{\partial z} - \frac{1}{c^2}\frac{\partial^2\overline{\psi}(x,z,\tau)}{\partial\tau^2} = 0. \tag{34}$$

6 Propagation of the Gaussian beam and of the Gaussian wave-packet in parabolic approximation

For the initial Gaussian-like wave-amplitude profile

$$\varphi_0(x) = \exp\left(-x^2/2W_{x0}^2\right) \tag{35}$$

with the spatial spectrum [1, 2]

$$\Phi_0(q) = W_{x0}\exp\left(-q^2W_{x0}^2/2\right)\Big/\sqrt{2\pi} \tag{36}$$

one obtains for the propagating monochromatic Gaussian beam wave from (27) the expression

$$\overline{\varphi}(x,z) = \frac{1}{\sqrt{1-j\alpha_0 z}}\exp\left\{-\frac{\beta_0}{2}\frac{\alpha_0 x^2}{(1-j\alpha_0 z)}\right\}, \tag{37}$$

where $\alpha_0 = 1/\beta_0 W_{x0}^2 = \lambda_0/2\pi W_{x0}^2$. The last formula can be written also as

$$\overline{\varphi}(x,z) = \frac{1}{\sqrt{1-j\alpha_0 z}}\exp\left\{-\frac{x^2}{2W_x^2}\right\}\exp\left\{j\beta_0\frac{x^2}{2R_x}\right\}, \tag{38}$$

where $W_x = W_{x0}\sqrt{1+(\alpha_0 z)^2}$ is the effective width of the beam wave and $R_x = -z\left[1+1\Big/(\alpha_0 z)^2\right]$ is the radius of the wave-front curvature (curvature of equi-phase surfaces) on the z-axis, both in the plane $z = const$. Both are functions of the propagation path z, *ie* $W_x = W_x(z)$, $R_x = R_x(z)$. In the plane $z = 0$ - the position of the beam waist - the effective radius $W_x = W_{x0}$ reaches its minimum and the wavefront is planar, *ie* the radius of equiphase surfaces R_x converges to infinity. For $z > 0$ the beam wave diverges, $R_x < 0$, while for $z < 0$ the wave is focused, $R_x > 0$.

In the near-zone of the beam waist, $\alpha_0 z << 1$, $z << W_{x0}^2/\lambda_0$, the wavefront is nearly planar ($|R_x| >> |z|$) - in fact the wave is effectively a plane wave with the Gaussian amplitude profile. In the far-zone of the beam waist, $\alpha_0 z >> 1$, $z >> W_{x0}^2/\lambda_0$, the wave in the paraxial region $|x| << |z|$ is effectively a spherical wave ($R_x \approx -z$) with the Gaussian amplitude profile and with the wave front curvature equal to the distance z from the beam waist.

In a special case of a spatio-temporal wave-packet, *ie* of a Gaussian distribution of the amplitude-envelope in time and space

$$\psi_0(x,t) = \exp\left(-x^2/2W_{x0}^2\right)\exp\left(-t^2/2W_{t0}^2\right) \tag{39}$$

with the spatio temporal spectrum

$$\Psi_0(q,\Omega) = W_{x0}W_{t0}\exp\left(-q^2W_{x0}^2/2\right)\exp\left(-\Omega^2W_{t0}^2/2\right)/2\pi, \tag{40}$$

formula (31) yields a product of two single, one spatial and one temporal inverse Fourier integrals

$$\begin{aligned}\overline{\psi}(x,z,t-z/c) = {}& \frac{W_{x0}W_{t0}}{2\pi}\times \\ &\times\int_{-\infty}^{\infty}\exp\left(\frac{-q^2W_{x0}^2}{2}\right)\exp\left\{\frac{jzq^2}{2\beta_0}\right\}\exp\{-jqx\}\mathrm{d}q\times \\ &\times\int_{-\infty}^{\infty}\exp\left(\frac{-\Omega^2W_{t0}^2}{2}\right)\exp\left\{-\frac{jz\Omega^2}{2c^2\beta_0}\right\} \\ &\times\exp\{j\Omega(t-z/c)\}\,\mathrm{d}\omega,\end{aligned} \tag{41}$$

with the result

$$\begin{aligned}\overline{\psi}(x,z,t-z/c) = {}& \frac{1}{\sqrt{1-j\alpha_0 z}}\exp\left\{-\frac{\beta_0}{2}\frac{\alpha_0 x^2}{(1-j\alpha_0 z)}\right\}\times \\ &\times\frac{1}{\sqrt{1+j\chi_0 z}}\exp\left\{-c^2\frac{\beta_0}{2}\frac{\chi_0(t-z/c)^2}{(1+j\chi_0 z)}\right\},\end{aligned} \tag{42}$$

where $\chi_0 = 1/c\omega_0 W_{t0}^2 = 1/\beta_0\left(cW_{t0}\right)^2$.

The first part of (42) is in fact the amplitude distribution of the monochromatic beam wave identical with (37). The second part denotes a retarded temporal Gaussian pulse that can be written in analogy with (38) in the form

$$\frac{1}{\sqrt{1+j\chi_0 z}}\exp\left\{-\frac{(t-z/c)^2}{2W_t^2}\right\}\exp\left\{jc^2\beta_0\frac{(t-z/c)^2}{2R_t}\right\}, \tag{43}$$

where the effective width of the pulse in time domain is $W_t = W_{t0}\sqrt{1+(\chi_0 z)^2}$, and $R_t = z\left[1+1\Big/(\chi_0 z)^2\right]$ characterises the non-linear phase modulation (chirping) of the pulse. Both are functions of the propagation path z, *ie* $W_t = W_t(z)$, $R_t = R_t(z)$.

The chirping of the carrier frequency means that the instantaneous carrier frequency instead of ω_0 equals

$$\omega(t,z) = \omega_0\left[1+(ct-z)/R_t\right]. \tag{44}$$

The final formula for the electric intensity takes either the form

$$\mathbf{E}(\mathbf{r},t) = \mathrm{Re}\left\{\mathbf{u}_y E_0\overline{\varphi}(x,z)\exp\left[j\left(\omega_0 t-\beta_0 z\right)\right]\right\} \tag{45}$$

for Gaussian beam, or

$$\mathbf{E}(\mathbf{r},t) = \mathrm{Re}\left\{\mathbf{u}_y E_0\overline{\psi}(x,z,t-z/c)\exp\left[j\omega_0\left(t-z/c\right)\right]\right\}. \tag{46}$$

for the Gaussian wave-packet.

If one considers (38) and (43) it is easily seen, that the profile of the wave intensity is a symmetrical Gaussian function for the transversal variable x and also for the time variable t. However, the longitudinal intensity profile as a function of the variable z is not symmetrical, *ie* is given as

$$\begin{aligned}\left|\overline{\psi}(x,z,t-z/c)\right|_{x=0}^2 = {}& \frac{1}{\sqrt{\left(1+\alpha_0^2z^2\right)\left(1+\chi_0^2z^2\right)}}\times \\ &\times\exp\left\{-\frac{(t-z/c)^2}{W_{t0}^2\left(1+\chi_0^2z^2\right)}\right\},\end{aligned} \tag{47}$$

as seen in Fig. 1(a),(b),(c) and Fig. 2.

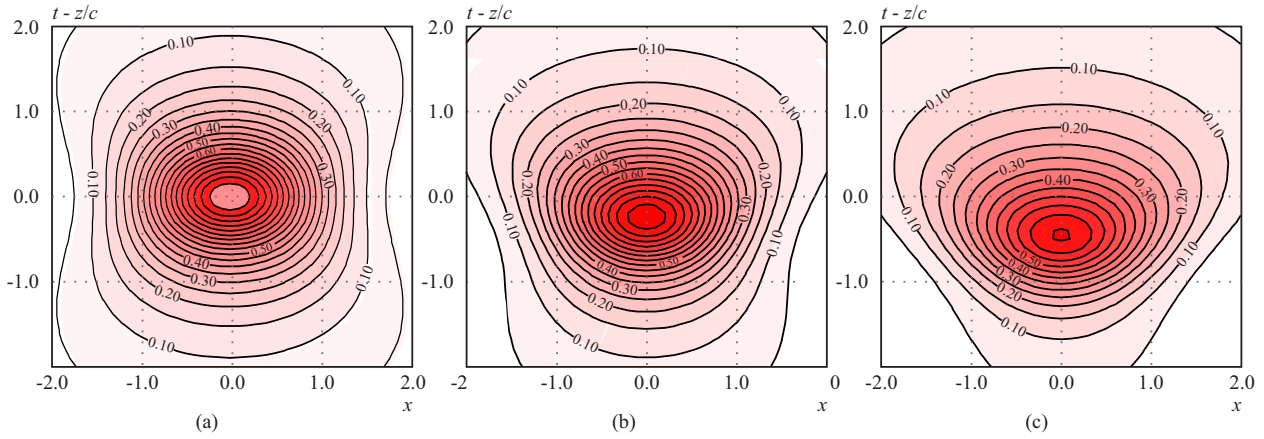

Fig. 1. Contour lines of intensity profiles accordingly (42) for $\alpha_0 = 1$, $\chi_0 = 1$, $W_{t0} = 1$, $W_{x0} = 1$ and for (a): $t_1 = 0$, (b): $t_2 = 0.5$ and (c): $t_3 = 1$

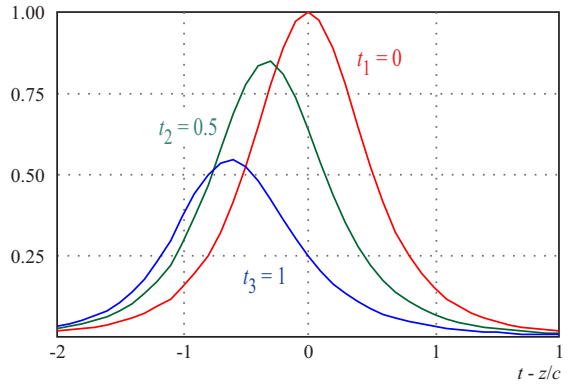

Fig. 2. Profiles of (47), *ie* a cut through Fig.1 contours at $x = 0$, for $\alpha_0 = 1$, $\chi_0 = 1$, $W_{t0} = 1$ for (a): $t_1 = 0$ (red), (b): $t_2 = 0.5$ (green) and (c): $t_3 = 1$ (blue)

7 Some aspects of the numerical implementation

7.1 Sampling of the spectral densities and interpolation of the wave amplitude

In the numerical modelling only certain limited number, either even $2N$, or odd $2N+1$, of discretised values of harmonics $\Phi_{0n} = \Phi_0(q_n)$ of the initial condition $\varphi_0(x) \leftrightarrow \Phi_0(q)$, or $\Phi_n(z) = \Phi(q_n, z)$ of the solution $\varphi(x,z) \leftrightarrow \Phi(q,z)$, can be used, where $q_n = nq_0$ and q_0 is the basic spatial frequency, with $n \in \{-N+1, N\}$ for the even and $n \in \{-N, N\}$ for the odd number of discretised values.

The periodic band-limited function $\widetilde{\varphi}_0(x)$ obtained by using the Fourier series for even or odd number of Φ_{0n} values, *ie*

$$\widetilde{\varphi}_0(x) = \sum_{n=-N+1}^{N-1} \Phi_{0n} \exp(-jnq_0x) + \Phi_{0N} \cos(Nq_0x), \tag{48}$$

or

$$\widetilde{\varphi}_0(x) = \sum_{n=-N}^{N} \Phi_{0n} \exp(-jnq_0x) \tag{49}$$

is used, instead of the inverse Fourier transform in form of (11). It approximates $\varphi_0(x)$ on the interval $(-x_{\max}, x_{\max})$, where $x_{\max} = \pi/q_0$.

The sampled values $\widetilde{\varphi}_{0k} = \widetilde{\varphi}_0(x_k)$ in the points $x_k = k\Delta_x$, where $\Delta_x = x_{\max}/N$, $k \in \{-N+1, \cdots, N\}$ are obtained for the even number $2N$ using (48)

$$\widetilde{\varphi}_{0k} = \sum_{n=-N+1}^{N} \Phi_{0n} \exp\{-j\pi kn/N\}. \tag{50}$$

Similarly, the sampled values $\widetilde{\varphi}_{0k} = \widetilde{\varphi}_0(x_k)$ for the odd number $2N+1$ of sampling points $x_k = \left(k - \frac{1}{2}\right)\Delta_x$, $k \in \{-N, \cdots, N\}$, where $\Delta_x = x_{\max}/\left(N + \frac{1}{2}\right)$ are obtained, using (49)

$$\widetilde{\varphi}_{0k} = \sum_{n=-N}^{N} \Phi_{0n} \exp\left\{-j2\pi\left(k - \tfrac{1}{2}\right)n/(2N+1)\right\}. \tag{51}$$

Both (50) and (51) exactly correspond to the definition of the inverse discrete Fourier transform. Therefore also

$$\Phi_{0n} = \frac{1}{2N} \sum_{k=-N}^{N-1} \widetilde{\varphi}_{0k} \exp\{j\pi kn/N\}, \tag{52}$$

for the even, and

$$\Phi_{0n} = \frac{1}{2N+1} \sum_{k=-N}^{N} \widetilde{\varphi}_{0k} \exp\left\{j2\pi\left(k - \tfrac{1}{2}\right)n/(2N+1)\right\}, \tag{53}$$

for the odd number of samples.

Substituting (52) into (48) and (53) into (49) interchanging the order of summation and summing the geometrical series with respect to n yields [2] either

$$\widetilde{\varphi}_0(x) = \frac{1}{2N} \sum_{k=-N+1}^{N-1} (-1)^k \widetilde{\varphi}_{0k} \times \\ \times \sin(Nq_0x) \cot\left\{\tfrac{1}{2}(q_0x - \frac{\pi k}{N})\right\} \tag{54}$$

for the even number of the sampling points, or

$$\widetilde{\varphi}_0(x) = \frac{1}{2N+1} \sum_{k=-N}^{N} \widetilde{\varphi}_{0k} \sin\left\{(N+\tfrac{1}{2})q_0x \right. \\ \left. - \pi(k - \tfrac{1}{2})\right\} \Big/ \sin\left\{\tfrac{1}{2}q_0x - \frac{\pi(2k-1)}{4N+2}\right\} \tag{55}$$

for the odd one respectively.

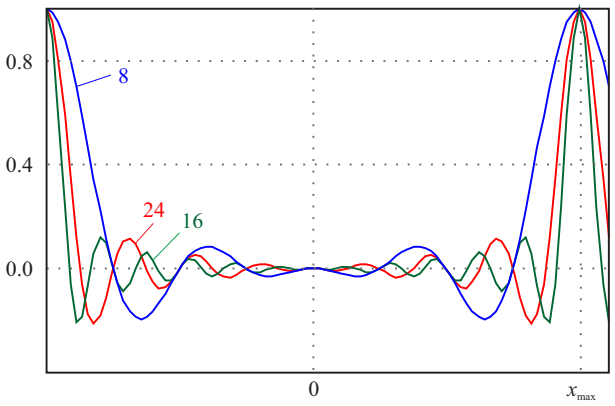

Fig. 3. Kernel function (56) for: 2N = 8, 16, 24

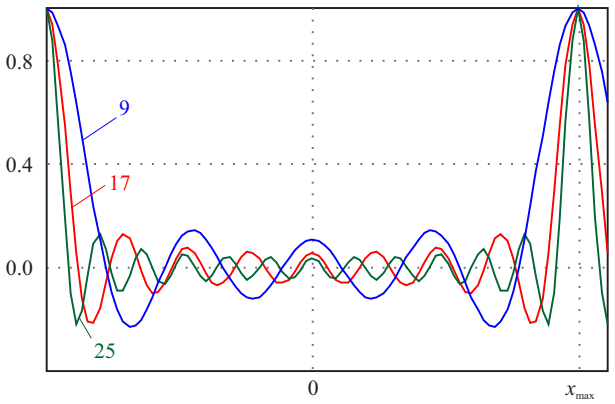

Fig. 4. Kernel function (57) for: 2N +1 = 9, 17, 25

Both formulae (54) and (55) in fact mean an interpolation of the bandlimited function $\widetilde{\varphi}_0(x)$ between its sampled values $\widetilde{\varphi}_{0k}$ in the sampling points equal either $x_k = k\Delta_x$, or $x_k = \left(k - \frac{1}{2}\right)\Delta_x$. The kernel functions of interpolation either for the even number of samples $2N$

$$(-1)^k \sin(Nq_0x)\cos\left(\frac{1}{2}q_0x\right)\Big/ 2N\sin\left(\frac{1}{2}q_0x\right), \quad (56)$$

or for the odd number of samples $2N+1$

$$\sin\left\{\left(N+\frac{1}{2}\right)q_0x\right\}\Big/(2N+1)\sin\left\{\frac{1}{2}q_0x\right\}, \quad (57)$$

are illustrated in Fig. 3 and Fig. 4. The figures indicate that the oscillatory character of interpolation functions is smaller for even number of interpolating points than for odd.

7.2 Boundary conditions

In the boundary points of the computational window the boundary conditions must be formulated. The so-called "electric wall" is represented by zero boundary values $\widetilde{\varphi}_0(x) = 0$ in points $x = 0$ and $x = x_{max}$, and the so-called "magnetic wall" by zero derivatives $\partial\widetilde{\varphi}_0(x)/\partial x = 0$ in the same boundary points. In such cases the function $\widetilde{\varphi}_0(x)$ becomes either an even, or an odd function on the interval of the period $(-x_{max}, x_{max})$, and (49) (for the odd number of samples $2N+1$) can be expressed either in the form

$$\widetilde{\varphi}_0(x) = \Phi_{00} + \sum_{n=1}^{N} 2\Phi_{0n}\cos(nq_0x) \quad (58)$$

for the "electric wall", since $\Phi_{0(-n)} = \Phi_{0n}$, or in the form

$$\widetilde{\varphi}_0(x) = \sum_{n=1}^{N} 2j\Phi_{0n}\sin(nq_0x) \quad (59)$$

for the "magnetic wall", since $\Phi_{0(-n)} = -\Phi_{0n}$.

Since usually a symmetric initial amplitude distribution within the computational window $(0, x_{max})$ is used, *ie* $\widetilde{\varphi}_0(x_{max}/2 + x) = \widetilde{\varphi}_0(x_{max}/2 - x)$, then in (58) only the terms with even n occur, and in (59) only the terms with odd n. The case of the even number of samples $2N$ is analogous using (48) instead of (49), but for the sake of brevity not shown here.

Similar situation occurs also for $\psi_0(x,t) \Leftrightarrow \Psi_0(q,\Omega)$, since for the numerical modelling only a finite number of spatial and temporal harmonics can be used, *ie* the set of discrete values $\Psi_{0(n,m)} = \Psi_0(nq_0, m\Omega_0)$, $n \in \{-N, N\}$, $m \in \{-M, M\}$, instead of continuous $\Psi_0(q,\Omega)$. In analogy to (49) the double periodic band-limited function $\widetilde{\psi}_0(x,t)$

$$\widetilde{\psi}_0(x,t) = \sum_{m=-M}^{M}\sum_{n=-N}^{N} \Psi_{0(n,m)}\exp\left[j\left(m\Omega_0t - nq_0x\right)\right] \quad (60)$$

approximates $\psi_0(x,t)$ in the computational window $(0, x_{max}) \times (0, t_{max})$, where $x_{max} = \pi/q_0$, $t_{max} = \pi/\Omega_0$.

Taking the values on the boundaries of computational window as electric walls or magnetic walls one arrives again to double sums

$$\widetilde{\psi}_0(x,t) = \Psi_{00} + \sum_{m=1}^{M}\left\{\sum_{n=1}^{N} 2\Psi_{n,m}\cos(nq_0x)\right\}\cos(m\Omega_0t), \quad (61)$$

$$\widetilde{\psi}_0(x,t) = \sum_{m=1}^{M}\left\{\sum_{n=1}^{N} 2j\Psi_{n,m}\sin(nq_0x)\right\}\sin(m\Omega_0t). \quad (62)$$

7.3 Amplitude of the propagating wave

The resulting $\widetilde{\varphi}(x,z)$ is then for *eg* odd number of samples $2N+1$ obtained either as

$$\widetilde{\varphi}_0(x,z) = \Phi_{00}\exp(-j\beta_0z) + \\ + \sum_{n=1}^{N} 2\Phi_n\exp\left(-jz\sqrt{\beta_0^2 - n^2q_0^2}\right)\cos(nq_0x), \quad (63)$$

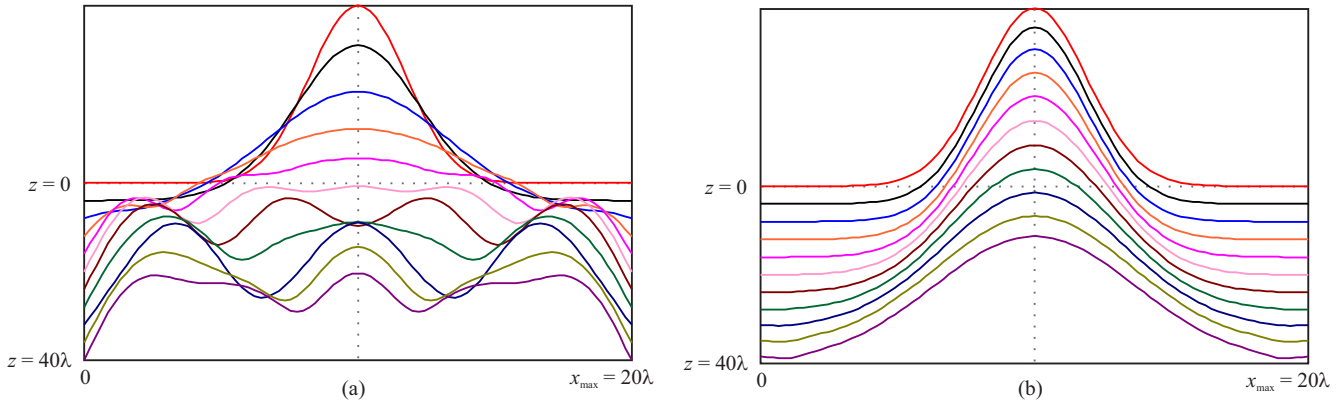

Fig. 5. Propagation of the smooth-impulse monochromatic beam-wave along the propagation path of $40\,\lambda$ with the window width of $20\,\lambda$: (a) – the electric walls, and (b) – the magnetic walls

for the "electric wall", or as

$$\widetilde{\varphi}_0\,(x,z) = \sum_{n=1}^{N} 2j\Phi_{0n} \exp\left(-jz\sqrt{\beta_0^2 - n^2 q_0^2}\right) \sin\left(nq_0 x\right) \tag{64}$$

for the "magnetic wall".

For the spatio-temporal pulse the discrete version of (23) using (61) for the electric wall yields

$$\widetilde{\psi}_0\,(x,z,t) = \Psi_{00} \exp\left(-j\beta_0 z\right) + \sum_{m=1}^{M} \left\{ \sum_{n=1}^{N} 2\Psi_{n,m} \times \right.$$

$$\left. \times \exp\left(-jz\sqrt{\left[\beta_0 + m\Omega_0/c\right]^2 - n^2 q_0^2}\right) \cos\left(nq_0 x\right) \right\} \times$$

$$\times \cos\left(m\Omega_0 t\right). \tag{65}$$

Similar result can be obtained using (62) for the magnetic wall.

Observe that the function $\exp\left(-jz\cdots\right)$ in the double sum of (65) is even for n, *ie* it has the same value for $\pm n$, but it is not even for m. This leads to an unsymmetry in the wave-amplitude-profile with respect to the variable z as already pointed out in (47) concerning the parabolic approximation.

7.4 Design of the initial impulse

The periodic smooth-impulse function has been constructed as follows. On the interval $(0, x_{\max})$ we construct an symmetric function $\widetilde{\varphi}_0(x_{\max}/2 - x) = \widetilde{\varphi}_0(x_{\max}/2 + x)$ such that in the boundary points all derivatives of the function are zero. On the interval $(-x_{\max}, x_{\max})$ this function can be taken either even (magnetic wall), or odd (electric wall), *ie* either $\widetilde{\varphi}_0(-x) = \widetilde{\varphi}_0(x)$, or $\widetilde{\varphi}_0(-x) = -\widetilde{\varphi}_0(x)$.

For the magnetic wall one obtains

$$\widetilde{\varphi}_0(x) = \sum_{n=0}^{N} a_n \cos\left(n\Delta_q x\right) \Big/ \sum_{n=0}^{N} a_n\,, \tag{66}$$

where odd a_n are zero and even a_n are solutions of the set of equations

$$\sum_{n=2}^{N} (-1)^n n^{2k} a_n = 1,$$

$$k = 1, 2, \cdots, N-1, \qquad a_0 = -\sum_{n=1}^{N} a_n. \tag{67}$$

Herewith the even periodic function $\widetilde{\varphi}_0(x)$ is normalised to maximum value one, $\widetilde{\varphi}_0(0) = 1$, and equal to zero in the computational window boundary points, $\widetilde{\varphi}_0(0) = \widetilde{\varphi}_0(x_{\max}) = 0$ with the zero derivatives in the same points up to the order N.

For the electric wall one constructs an odd function on the interval $(-x_{\max}, x_{\max})$, defining the smooth-impulse curve within the computational window, *ie* on the half-period interval $(0, x_{\max})$ as

$$\widetilde{\varphi}_0(x) = \sum_{n=0}^{N} b_n \sin(n\Delta_q x) \Big/ \sum_{n=0}^{N} b_n\,, \tag{68}$$

where even b_n are zero and b_n are solutions of the set of equations

$$\sum_{n=2}^{N} (-1)^n n^{2k-1} b_n = 1,$$

$$k = 1, 2, \cdots N-1, \quad b_0 = 0. \tag{69}$$

Herewith the odd periodic function $\widetilde{\varphi}_0(x)$ with the zero derivatives in the boundary points up to the order N, is again normalised to maximum value one, $\widetilde{\varphi}_0(0) = 1$, and equal to zero in the boundary points, $\widetilde{\varphi}_0(0) = \widetilde{\varphi}_0(x_{\max}) = 0$.

In Table 1 and Table 2 the amplitudes of harmonic components are shown for the various maximum number N. As can be seen from Table 3 they are nearly identical with the harmonic components taken from the Gaussian-shape spectral density. On the other hand the width of the smooth-impulse function with respect to window width cannot be arbitrarily changed as it is the case for the Gaussian impulse.

Table 1. Harmonic components for the electric wall smooth-impulse function

n	1	3	5	7	9	11	13
N							
7	0.547	-0.328	0.0598	-0.0156			
l9	0.492	-0.328	0.1410	-0.0352	0.00391		
11	0.451	-0.322	0.1610	-0.0537	0.01070	-0.000977	
13	0.419	-0.314	0.1750	-0.0698	0.01900	-0.003170	0.000244

Table 2. Harmonic components for the magnetic wall smooth-impulse function

n	0	2	4	6	8	10	12
N							
8	0.273	0.219	0.0625	0.00781			
l0	0.246	0.234	0.0879	0.01950	0.00195		
12	0.226	0.242	0.1070	0.03220	0.00586	0.000488	
14	0.209	0.244	0.1220	0.04440	0.01110	0.001710	0.000122

Table 3. Harmonic components for the magnetic wall as defined by Gaussian-shape spectral density

n	0	2	4	6	8	10	12
N							
14	0.207	0.362	0.242	0.123	0.0478	0.00321	0.000556

7.5 Boundary reflection effects

Since in the course of propagation the impulse broadens the significant reflection effects on the boundaries occur. Another interpretation of these effects is that, since in fact one deals with the periodic function, the tails of the broadened impulse penetrate into the computational window from the neighbouring periodic windows. Therefore these effects are completely different for the electric and magnetic walls respectively.

As it is easily seen from Fig. 5, the electric walls have much more deteriorating effect on the beam-wave envelope profile than the magnetic walls.

8 Conclusions

Some aspects and critical features of the two-dimensional-wave-packet propagation had been thoroughly discussed. The results will be used in subsequent papers concerning the passing the wave-packet through dielectric boundaries, transient Goose-Hänchen shift and transient frustrated total internal reflection.

Acknowledgements

The financial support of this work from the VEGA grant agency under the project No. 1/0405/16 is kindly acknowledged.

References

[1] O. N. Litvinenko, *Osnovy radiooptiky*, (Basics of radio-optics) Izd. "Technika", Kiev 1974, (in Russian).

[2] A. Papoulis, *Systems and Transforms with Applications in Optics*, McGraw Hill, New York 1968.

Received 10 December 2016

Ľubomír Šumichrast is with the Faculty of Electrical Engineering and Information Technology of the Slovak University of Technology since 1971, now holding the position of an Associate Professor and Deputy director of the Institute of Electrical Engineering. He spent the period 1990-1992 as a visiting professor at the University Kaiserslautern, Germany and spring semester 1999 as a visiting professor at the Technical University Ilmenau, Germany. His main research interests include the electromagnetic waves propagation in various media and structures, computer modelling of wave propagation effects as well as optical communication and integrated optics.

Jaroslav Franek (Ing, CSc), was born in Bratislava, former Czechoslovakia, in 1946. He graduated from the Faculty of Electrical Engineering, Slovak Technical University, Bratislava from solid state physics branch, in 1969, and received the CSc (PhD) degree in Physics in 1986. At present he is with the Institute of Electrical Engineering at his Alma Mater. The main fields of his research and teaching activities are circuit and electromagnetic field theory, namely the microwave technology.